

## Understanding Species Boundaries that Arise from Complex Histories: Gene Flow Across the Speciation Continuum in the Spotted Whiptail Lizards

ANTHONY J. BARLEY<sup>1,\*</sup> , ADRIÁN NIETO-MONTES DE OCA<sup>2</sup>, NORMA L. MANRÍQUEZ-MORÁN<sup>3</sup>, AND ROBERT C. THOMSON<sup>4</sup> 

<sup>1</sup>School of Mathematical and Natural Sciences, Arizona State University, West Valley Campus, 4701 W Thunderbird Road, Glendale, AZ 85306, USA

<sup>2</sup>Laboratorio de Herpetología and Museo de Zoología Alfonso L. Herrera, Departamento de Biología Evolutiva, Facultad de Ciencias, Universidad Nacional Autónoma de México, Cd. Universitaria, Del. Coyoacán, Ciudad de México, C.P. 04510, México

<sup>3</sup>Laboratorio de Sistemática Molecular, Centro de Investigaciones Biológicas, Universidad Autónoma del Estado de Hidalgo, Km. 4.5 Carr. Pachuca-Tulancingo, Col. Carboneras, Mineral de la Reforma, Hidalgo, C.P. 42184, México

<sup>4</sup>School of Life Sciences, University of Hawai'i, 3190 Maile Way, Honolulu, HI 96822, USA

\*Correspondence to be sent to: School of Mathematical and Natural Sciences, Arizona State University—West Valley Campus, 4701 W Thunderbird Road, Glendale, AZ 85306, USA; E-mail: [ajbarley@asu.edu](mailto:ajbarley@asu.edu)

Received 12 February 2024; accepted 17 July 2024

Associate Editor: Bryan Carstens

**Abstract.**—Gene flow between diverging lineages challenges the resolution of species boundaries and the understanding of evolutionary history in recent radiations. Here, we integrate phylogenetic and coalescent tools to resolve reticulate patterns of diversification and use a perspective focused on evolutionary mechanisms to distinguish interspecific and intraspecific taxonomic variation. We use this approach to resolve the systematics for one of the most intensively studied but difficult to understand groups of reptiles: the spotted whiptail lizards of the genus *Aspidoscelis* (*A. gularis* complex). Whiptails contain the largest number of unisexual species known within any vertebrate group and the spotted whiptail complex has played a key role in the generation of this diversity through hybrid speciation. Understanding lineage boundaries and the evolutionary history of divergence and reticulation within this group is therefore key to understanding the generation of unisexual diversity in whiptails. Despite this importance, long-standing confusion about their systematics has impeded understanding of which gonochoristic species have contributed to the formation of unisexual lineages. Using reduced representation genomic data, we resolve patterns of divergence and gene flow within the spotted whiptails and clarify patterns of hybrid speciation. We find evidence that biogeographically structured ecological and environmental variation has been important in morphological and genetic diversification, as well as the maintenance of species boundaries in this system. Our study elucidates how gene flow among lineages and the continuous nature of speciation can bias the practice of species delimitation and lead taxonomists operating under different frameworks to different conclusions (here we propose that a 2 species arrangement best reflects our current understanding). In doing so, this study provides conceptual and methodological insights into approaches to resolving diversification patterns and species boundaries in rapid radiations with complex histories, as well as long-standing taxonomic challenges in the field of systematic biology. [Aspidoscelis; hybridization; parthenogenesis; phylogenetic networks; RADseq.]

*“Most of the ‘species’ are so plastic, so variable, that they may well drive the systematist to despair. No two taxonomic authorities will, or can, possibly agree on the number of admissible species.”* - Hans Gadow (1906) discussing the systematics of Mexican whiptail lizards.

Hybridization and gene flow during evolutionary divergence cause numerous challenges for the inference of evolutionary history. In the case of recent allopatric or parapatric divergence, it can generate geographically separated, phenotypically distinctive populations between which relationships and lineage boundaries are difficult to identify. These systems require accurate inference of the processes that contributed to lineage divergence if we wish to delimit species robustly (Dufresnes et al. 2020, 2023; Chambers et al. 2023). Inference under phylogenetic models that do not account for gene flow when it is present may underestimate divergence times between lineages (Leaché et al. 2014) and lead to underestimation of species-level diversity itself. Alternatively, if systematists accept the overwhelming evidence for

gene flow between distinct species, this can result in species diversity being overestimated. This occurs because intraspecific genetic and phenotypic differentiation can generate patterns in the data that are similar to those produced by the process of speciation in the presence of gene flow, thereby leading to recognition of intraspecific variation as species. For example, isolation by distance, local adaptation, and phenotypic plasticity can cause correlated divergence in genetic and phenotypic traits across geographically localized populations, which is often used as evidence for species distinctiveness in integrative taxonomic frameworks (McLean and Stuart-Fox 2014; Barley et al. 2018; Hartop et al. 2022). The fact that speciation occurs at a wide range of rates and in the presence of gene flow makes it difficult to distinguish alternative biological processes based on observed patterns of genetic and phenotypic variation and generates the potential for taxonomists to ascribe species status to populations that are not on independent evolutionary trajectories (de Queiroz 2007).

Identifying species in the presence of gene flow is a contentious and difficult problem in systematic biology (Hillis et al. 2021). The general lineage species concept defines species as independently evolving metapopulation lineages (de Queiroz 1998). This requires that entities identified as species be on distinctive evolutionary trajectories, but does not preclude some gene flow occurring among them. Operationalizing the general lineage species concept involves identifying lineages that have sufficiently diverged to allow for speciation and do not freely exchange genes in sympatry. Lineages at intermediate levels of divergence, in which populations have experienced enough isolation for some differentiation to arise but it remains unclear if sufficient time has passed to ensure that speciation has occurred, are sometimes described as existing within the “speciation continuum” (Shaw and Mullen 2014; Galtier 2019). One way of making taxonomic progress in the face of these challenges is to model the evolutionary process that generated the diversity directly (Smith and Carstens 2020; Ramírez-Portilla and Quattrini 2023). In complex divergence scenarios, researchers need to understand not just the divergence times between lineages, but also rates of gene flow, which can vary continuously both in time and magnitude. This complicates matching empirical biological scenarios to the relatively simple inference models that have historically been available (Flouri et al. 2020). Ongoing model elaboration is relaxing this limitation over time and a variety of approaches are now available for making inferences about horizontal gene transfer between species and other complicating features of species level diversification processes (Mirarab et al. 2021; Hibbins and Hahn 2022). However, in nascent radiations, the distinction between recent population genetic and historical phylogenetic processes is often blurred, and the relative importance of tree versus network-based structures for understanding evolutionary history is often unknown. Thus, major unresolved issues in these systems include 1) how we should resolve the time-continuous, multifarious process of speciation to draw taxonomic conclusions about the nature of species boundaries and 2) how robustly we can resolve the historical patterns of branching and merging of lineages in groups of species that have complex evolutionary histories.

There are few taxonomic groups whose systematic history is characterized by as many difficulties in identifying boundaries between species as the North American whiptail lizards (genus *Aspidoscelis*). Following his systematic study of the group, the zoologist Edward Drinker Cope remarked that “The discrimination of the North American species of this genus is the most difficult problem in our herpetology” (Cope 1900). This pattern in part reflects the long fascination that systematists have had with this unique clade of squamates, which represent the group of vertebrates containing the largest number of unisexual species. It also appears to be a consequence of the ubiquitous nature of hybridization among these lizards, which has

resulted in numerous examples of 2 distinct biological outcomes: introgressive hybridization between gonochoristic (i.e., sexual) species and hybrid speciation resulting in the formation of unisexual species (Barley et al. 2022a). Hybrid speciation between different pairs of gonochoristic species has generated a suite of unisexual species that represent approximately one third of all whiptail lizard diversity (Wright 1993). The taxonomic difficulties systematists have encountered in the clade also reflect the extraordinary patterns of phenotypic variation (e.g., in scalation and coloration phenotypes) that whiptail lizards exhibit within and between populations. In stark contrast to this variation, across other morphological and ecological axes of diversity, whiptail species exhibit substantial conservatism: virtually all species are diurnal, terrestrial insectivores with broadly similar habitats and ecologies. The final complicating factor to understanding diversity in these lizards is that intergradation (in both phenotypes and genetics) between populations within many whiptail species complexes is widespread, even when strikingly divergent populations have been identified in different regions (Duellman and Zweifel 1962; Barley et al. 2019).

Among the gonochoristic whiptail lizards, difficulties resolving species boundaries are perhaps best exemplified by the spotted whiptail lizards (i.e., the *A. gularis*/*A. septemvittatus* species complex; here we use the former, older name to refer to these lizards). Among populations of these lizards in different geographic regions of Mexico and the southwestern United States, dorsal, and ventral phenotypes are strikingly divergent (Fig. 1). This has resulted in the description of at least 8 different taxa that have at different times been considered species or subspecies (Table 1). Intergradation in intervening regions has caused marked confusion as to the significance of this variation, and the assignment of many populations within virtually any proposed taxonomic framework has proven problematic (Walker 1981a, b; Walker et al. 2001). For example, in a previous taxonomic revision of the *A. gularis* complex, Duellman and Zweifel (1962) noted “We can offer no assurance that all the lizards we refer to *Cnemidophorus septemvittatus* belong to the same species or even, if they do, that *septemvittatus* is the correct name.”

Beyond the intriguing nature of this phenotypic variation and the evolutionary processes that have produced it, this complex of lizards is among the most important for understanding the evolution of unisexuality in whiptails. Unisexual whiptail lineages initially form when the diploid, female F1 hybrid offspring of divergent sexual species reproduce parthenogenetically. Instantaneous hybrid speciation can also occur in these lizards through ploidy elevation when these diploid parthenogenetic clones secondarily backcross with a gonochoristic species (Barley et al. 2021). Populations within the *A. gularis* complex are thought to be one of the parental species for ~40% of the unisexual whiptail diversity. Therefore, testing theory related to why particular hybrid combinations induce reproductive

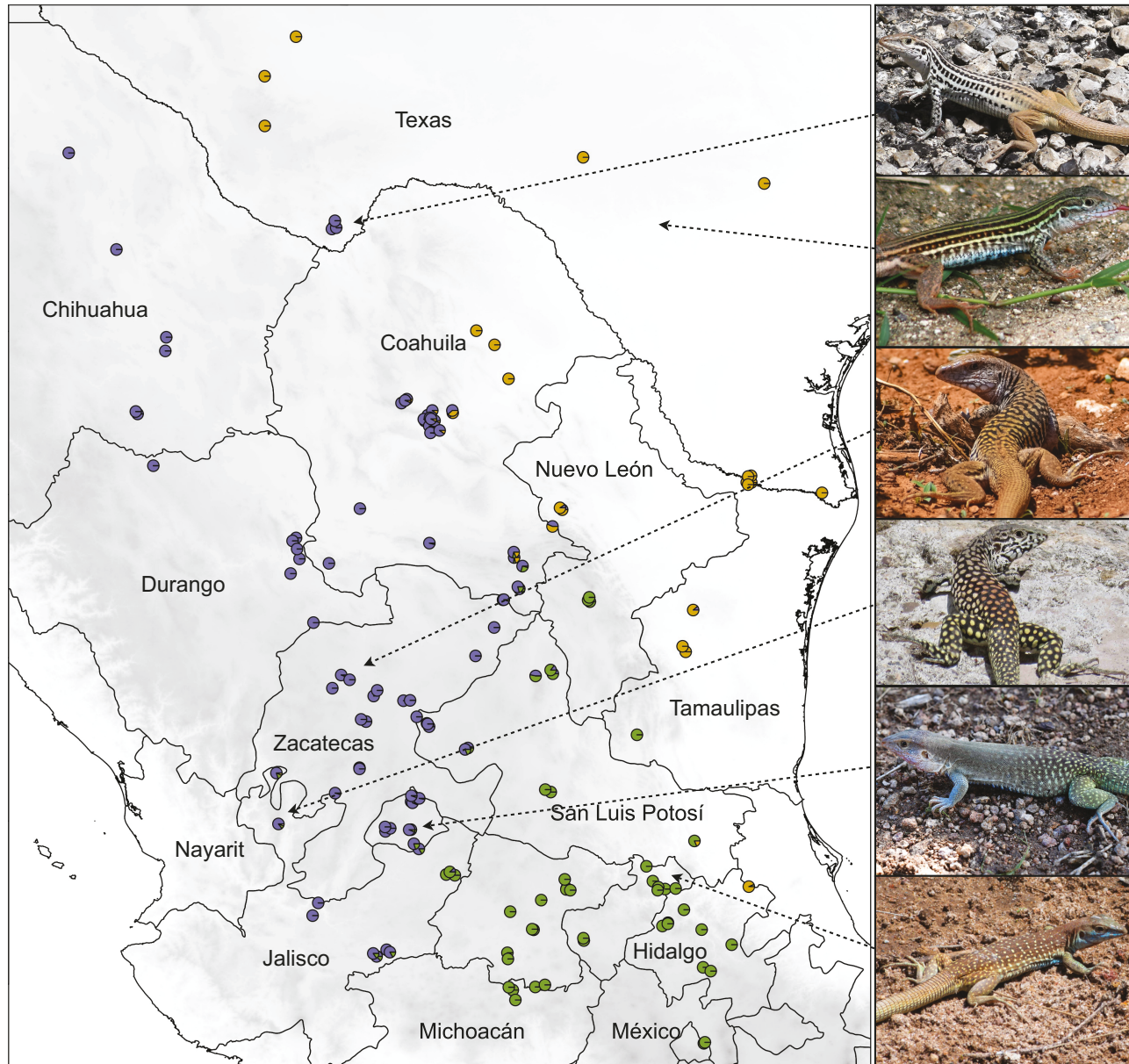


FIGURE 1. Map of sampling localities with pie charts illustrating genomic ancestry estimates from STRUCTURE analysis for  $K = 3$  with photos of populations from the *A. gularis* species complex. From top to bottom: *septemvittatus* from Terrell County, TX (photo Gary Nafis), *gularis* from Travis County, TX (photo Gary Nafis), *semiannulatus* from Zacatecas (photo Leonor Vázquez Rivera), undescribed population from Jalisco, Mexico (photo Emmanuel Guevara Lazcano), undescribed population from Aguascalientes, Mexico (photo AJB), and *rauni* from San Luis Potosí, Mexico (photo Luis Stevens).

mode transitions and developing mechanistic predictions to guide future studies of this phenomenon relies on understanding species boundaries and evolutionary history within the spotted whiptails (Moritz et al. 1989; Avise 2008). Presently, both the evolutionary diversity contained within the gonochoristic lineages in this complex and the ancestry of the unisexual lineages derived from it are not well understood.

Here, we develop a multi-step approach to resolve the systematics of taxonomic groups spanning the speciation continuum that exhibit complex evolutionary

histories (Fig. 2; see also Carstens et al. 2013; Chambers et al. 2023; Pyron et al. 2023; Pavón-Vázquez et al. 2024 for discussion of related ideas). The approach is focused on understanding the evolutionary processes that underly the systematic challenges in nascent radiations where hybridization, gene flow, and confusing patterns of geographically structured variation are present. The first step involves identifying metapopulation dynamics across the geographic landscape and the number of distinct populations within the radiation. We use both population genetic and phylogenetic tools

TABLE 1. Summary of taxonomic diversity within *A. gularis* species complex based on morphological study

Taxon	Type locality	Adult color pattern	GAB	FP	Distribution
<i>gularis</i> Baird and Girard 1852	Indianola and the valley of the Rio Grande del Norte, USA	Light stripes with dark fields on dorsum, bluish-black venter with salmon-red unspotted throat. Includes several moderately distinctive morphotypes	86.9 (66–107)	32.9 (27–41)	Southeastern Texas / Oklahoma, USA; NE Mexico
<i>scalaris</i> Cope 1892	Mexican Plateau south of Chihuahua, MX	Vivid light bars, stripes and spots on black dorsum, purplish-blue venter. Includes numerous highly variable populations.	83.6 (72–98)	34.5 (29–42)	Chihuahua, MX
<i>septemvittatus</i> Cope 1892	Marfa, Texas, USA	Light dorsal stripes with small spots, white venter, black chin spots	84.6 (78–97)	38.2 (34–43)	Big Bend, Texas; N Coahuila, MX
<i>semifasciatus</i> Cope 1892	Agua Nueva, Coahuila, MX	Abrupt differentiation in dorsal pattern at midbody where stripes and bars anteriorly transition to gray coloration posteriorly with small white spots, venter bluish-gray with orange suffusion	88.1 (70–106)	37.1 (30–45)	Southern Coahuila, MX
<i>pallidus</i> Duellman & Zweifel 1962	Three miles W Cuatro Ciénelas, Coahuila, MX	Unicolor dorsum, unmarked, white venter	85.0 (71–96)	37.8 (35–43)	Cuatro Ciénelas Basin, Coahuila, MX
<i>rauni</i> Walker 1966	Four miles ESE Charco Blanco, San Luis Potosí, MX	Small light dorsal spots, purple-blue venter	87.8 (71–103)	36.5 (30–44)	Central San Luis Potosí, MX
<i>semiannulatus</i> Walker 1981b	Five km SE Guadalupe, Zacatecas, MX	Barred and spotted dorsal pattern, reddish-pink venter	84.7 (73–98)	34.4 (28–40)	S Durango, Zacatecas, N Aguascalientes, MX
<i>colossus</i> Dixon et al. 1971	25 km N Jalpan, Queretaro, MX	Spotted dorsum, blue venter, large maximum adult body size	92.4 (82–105)	37.1 (28–44)	Jalpan Valley, Queretaro, MX
undescribed ssp. Zweifel 1959	–	Fine light spots on dark ground color, no fusion to form lateral bars	85.6 (79–91)	36 (32–42)	Region of Guadalajara, Jalisco, MX

Note: There has long been confusion about whether these taxa correspond to species or subspecies, so here we simply list the specific epithets under taxon. Populations in different geographic regions in the complex can primarily be distinguished by 3 morphological traits: dorsal and ventral color pattern, the number of granular scales surrounding the body (GAB; counted in a row at the midpoint), and the number of femoral pores (FP). Data given are means and ranges compiled from Zweifel (1959), Walker (1966), Dixon et al. (1971), and Walker (1981b).

to resolve the multifaceted demographic processes that operate across the relevant scales of species diversification, and then synthesize these results with other information (e.g., phenotypic data) to resolve the number of detectable, biologically relevant units. This integration is important because different methods have different sensitivities to model violations, in some cases sampling scheme can influence analytical results, and different approaches interrogate different timescales. The primary goal here is to generate a preliminary hypothesis of species boundaries through integrative taxonomy that is biologically (i.e., evolutionarily) meaningful, even if it does encompass intraspecific diversity. The second step involves resolving patterns of relatedness, isolation, and gene flow among the identified lineages. When evolutionary histories are complex, employing multiple phylogenetic approaches can be important in resolving different aspects of tree-like or reticulate histories.

The final step involves identifying the mechanisms of divergence to distinguish between intraspecific and interspecific variation and using this understanding to generate taxonomic hypotheses. The value of this approach is that it places taxonomic decision-making within a framework that specifies how speciation

occurred, establishing a hypothesis that is easily amenable to further testing as additional data becomes available. Here, we do this using a combination of insights from genetic, ecological, and biogeographic data. For example, considering thresholds of divergence time can be informative about whether speciation has occurred if populations occur in allopatry. Alternatively, low rates of migration and fixed allelic differences can provide a standardized measure of the independence of lineages whether in allopatry or not. A variety of other sources of information, including more direct measures of reproductive isolation or selection against hybridization, such as hybrid zone data or coalescent modeling can also be used to confirm species status. Finally, measures of ecological or morphological differentiation may be useful to determine whether population variation is clinal (i.e., intraspecific) or discrete (more likely to be associated with speciation). We used this approach to resolve the patterns of lineage divergence in the spotted whiptails and then went on to clarify the patterns of hybrid speciation that have generated unisexual whiptail species diversity. Our results resolve the evolutionary history of both the gonochoristic and unisexual species in this group and clarify species boundaries and taxonomy, thereby contributing to the development of this unique

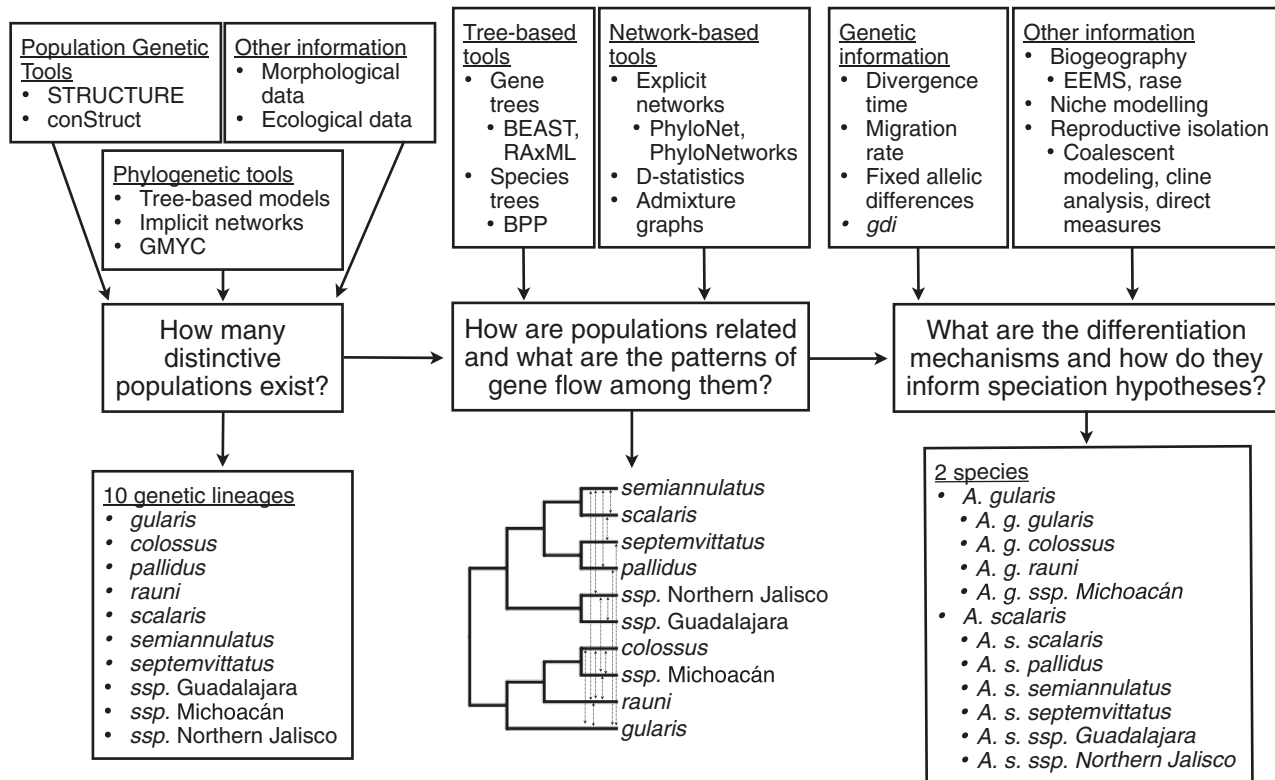


FIGURE 2. Outline of the approach for delimiting species in groups that have complex evolutionary histories. The major questions addressed through this approach are at the center and ordered from left to right. The top row outlines methods that we use in our study or that could be used to address the relevant question, and the bottom row summarizes the conclusions of our study.

group of vertebrates as a model for studying speciation and evolutionary transitions in reproductive mode.

## MATERIALS AND METHODS

### Sampling

We sampled populations of lizards within the *A. gularis* species complex across their distribution in the southwestern United States in Texas and Oklahoma, the Atlantic lowlands in northeastern Mexico, the Central Mexican Plateau, and the Trans-Mexican Volcanic Belt (Fig. 1). This sampling included numerous populations of all described species and subspecies in this complex, plus an additional undescribed form that has been discussed in the literature. Below, we refer to described taxa in this complex using the appropriate available epithet, although avoiding listing them as species (e.g., “*A. epithet*”) or subspecies (e.g., ‘*A. e. epithet*’) given the confusing nature of the taxonomy in this group, saving a discussion of our recommended taxonomy until the manuscript’s end. Samples of *A. costatus* were chosen to use as an outgroup in phylogenetic analyses because they represent the sister species to the *A. gularis* complex (Barley et al. 2022a). We also sampled populations of the unisexual *Aspidoscelis* species that are thought to have a hybrid parent within the *A.*

*gularis* complex and included samples of the alternative gonochoristic parent of these lineages, which are better understood (again based on the results of our previous work; Barley et al. 2022a). Newly collected specimens were deposited in the Museo de Zoología, Facultad de Ciencias, National Autonomous University of Mexico, and we included samples of several specimens previously deposited in museum collections (178 individuals in total; See [Supplementary Appendix 1](#) in Dryad repository for details).

We extracted DNA from tissue samples preserved in 100% ethanol or salt buffer using a variety of standard laboratory protocols. We built reduced representation genomic libraries using a restriction site associated DNA genotyping protocol (ddRADseq; Peterson et al. 2012; see Barley et al. 2019 for details). Sequencing for this work was done as part of a larger study and libraries were sequenced on several different Illumina platforms (the HiSeq 2500, HiSeq 4000, or NovaSeq 6000) using a single-end 100 base pair protocol. We performed a de novo assembly of the resulting read data using ipyrad v0.9.26 (Eaton and Overcast 2020). We identified an optimal clustering threshold value of 0.9, filtered out genotypes that had <10x coverage, and generated data sets for each analysis to minimize missing data and maximize power based on the individuals that were included and the computational constraints of the analysis. This involved subsampling from a set of

~20,000 RAD loci to generate data sets for analyses that were ~70–99% complete. Because ipyRAD cannot genotype polyploid individuals, we performed a de novo assembly of the data for the triploid parthenogenetic species in dDocent v2.7.8 to infer the ancestry of these lineages (Puritz et al. 2014). We used default parameters for this assembly with the same clustering similarity value and quality filtered variants using vcflib v1.0.2 (<http://github.com/ekg/vcflib>). To compare insights from the RADseq data to those derived from the mitochondrial (mtDNA) genome we downloaded the ND2 data from Esquivel-Ramírez et al. (2021) from Genbank and aligned the sequences using MUSCLE (Edgar 2004).

#### How Many Distinctive Populations Exist?

Our first goal was to characterize lineage diversity within the *A. gularis* complex to identify what would be considered the most permissive, biologically meaningful taxonomic hypothesis. To do this, we completed a literature review of phenotypic analyses that have been conducted for this species complex (Table 1) which we used in combination with both population genetic and phylogenetic analyses of the RADseq data to integrate metapopulation and tree-based perspectives on diversity. We first used the population genetic model STRUCTURE (Pritchard et al. 2000) to analyze the data set including all sampled individuals from the *A. gularis* complex. We used the admixture model, selected one single nucleotide polymorphism (SNP) per RAD locus, ran analyses for 100,000 generations following 100,000 generations of burn-in using default parameters, and explored varying numbers of populations (K) ranging from 2 to 8. The STRUCTURE model is sensitive to both hierarchical levels of genetic structure and allele frequency variation due to the geographically restricted nature of dispersal (i.e., isolation by distance). Therefore, we explored genetic variation within the primary genetic clusters we identified using STRUCTURE with conStruct (Bradburd et al. 2018). conStruct also uses allele frequencies to identify patterns of population structure, but models both continuous patterns of geographic variation and discrete genetic variation jointly (thus mitigating the potential that sampling gaps will cause clinal variation to be interpreted as lineage diversity). For each of the analyses, we used cross-validation to examine predictive accuracy scores across values of K between 1 and 7. We ran 3 replicates for each model using 10,000 iterations and visually checked for convergence using the parameter trace plots. After determining the optimal value of K for the spatial and nonspatial models, we ran a standard conStruct analysis under the same parameter settings to perform parameter estimation. To resolve patterns of genetic diversity within a phylogenetic framework, we performed a concatenated phylogenetic analysis. In this case, we also included the outgroup *A. costatus* samples and the full sequence data from each RAD locus. We performed this analysis within a Maximum Likelihood framework using RaxML v8.2.12 (Stamatakis 2014) on the CIPRES Science

Gateway with the automatic bootstrapping option and GTR+Γ model (Miller et al. 2010).

#### How Are Populations Related and What Are the Patterns of Gene Flow Among Them?

Based on previous studies and the genetic variation analyses, we expected the evolutionary history of these lizards to encompass both tree-like and reticulate components, so we used both standard phylogenetic models and phylogenetic network models to infer relationships among the lineages identified above. We also included analyses under numerous types of models due to the inherent tradeoffs that exist between different approaches, assumptions, and computational feasibility (i.e., no single model would likely represent the “best” approach to analyzing the data, but rather, different models might generate alternative insights into the biology of these species). The STRUCTURE analyses identified 3 primary genetic groups within the complex and suggested that several individuals in the data set derive a significant proportion of their ancestry from multiple of these genetic groups (likely due to hybridization/admixture). We suspect these represent early generation hybrids given the large proportion of genetic ancestry these individuals derive from each group. Therefore, we removed the 7 individuals that derived < 75% of their genetic ancestry from a single genetic group when performing subsequent phylogenetic analyses to make the data more consistent with the tree-like evolution assumptions of phylogenetic models (Pang and Zhang 2024).

We performed an outgroup-rooted, concatenated phylogenetic analysis of this data set using RaxML under the same parameterizations described above (and did the same for the ND1 mtDNA data set). We also performed a concatenated analysis of the data set (without the outgroup) in a Bayesian framework using the BEAST v.2.6.6 software (Bouckaert et al. 2014) to estimate relative divergence times. For this analysis, we used a GTR+Γ site model, a strict clock model, and default priors under the Coalescent Bayesian Skyline tree prior, running the analysis for 40 million generations, sampling every 4000 generations. In this and subsequent Bayesian analyses, we identified an appropriate burn-in value and checked for suitable mixing and convergence using Tracer v1.7.1 (Rambaut et al. 2018) by ensuring that all parameters had reached apparent stationarity and achieved an ESS > 1000. We performed a species tree analysis for 10 genetically cohesive lineages that we identified in the analyses exploring genetic variation in the previous section. We performed this analysis under the multispecies coalescent model (MSC) using the Bayesian Phylogenetics and Phylogeography (BPP) v.4.3.0 software (Rannala and Yang 2017). The data set for this analysis comprised 500 loci for 3 individuals (6 alleles) per lineage (preliminary analyses using larger number of loci showed poor mixing and did not reach convergence). We used largely default parameters under the A01 algorithm and

the auto-fine tuning option, set diffuse inverse gamma prior distributions on  $\theta$ -IG(3, 0.01) and  $\tau$ -IG(3, 0.04) (Campillo et al. 2020), and sampled the analysis every 100 iterations following 25,000 iterations of burnin for 10 million iterations.

We estimated levels of phylogenetic discordance attributable to introgression by calculating  $D$ - and  $F$ -branch statistics for the 10 *A. gularis* lineages using the Dsuite software (Malinsky et al. 2021). For these analyses, we assumed the topology from the concatenated BEAST analysis in the Dtrios and Fbranch programs and assessed support using the block jackknifing procedure. We also reconstructed evolutionary history using this data set with 2 phylogenetic network models (PhyloNet and PhyloNetworks) that jointly account for horizontal gene transfer and incomplete lineage sorting. For analyses using the PhyloNet software, we randomly selected a single SNP per RAD locus, included a single individual per lineage, and used the MLE\_BiMarkers model with the following arguments: MLE\_BiMarkers -pseudo -mnr 100 -mec 50000 -mno 10 -mf 50 -pi0 0.5 -diploid -mr 1 -ptheta 0.005 -thetawindow 0.005 (Zhu and Nahkleh 2018). We also ran a PhyloNet analysis under a 3-species model to estimate the relationships among the 3 primary genetic lineages we identified, because alternative analyses that included all the lineages were discordant in terms of how these primary lineages were related. Finally, we conducted a PhyloNet analysis that incorporated an eleventh population, previously described as *semifasciatus* based on morphological data, but that the STRUCTURE analysis indicated was comprised solely of admixed (recent generation hybrid) individuals to confirm support for this conclusion. We then estimated evolutionary networks using the PhyloNetworks software for the same taxonomic sampling used in PhyloNet (Solís-Lemus and Ané 2016). For these analyses, we included 3 individuals per lineage and calculated concordance factors from the SNP data using the SNPs2CF R function (Olave and Meyer 2020). We reconstructed maximum pseudolikelihood phylogenetic networks with 0–4 reticulations for the data set using the snaq! function. We performed 2 analyses for each model to ensure they converged to the same topologies, each with 100 runs. We evaluated the change in the negative log pseudolikelihood score as reticulation edges were added to identify the network with the optimal number of reticulations for the data set.

We observed substantial topological discordance across the phylogenetic approaches and used admixture graphs to compare support in the genomic data for the alternative topologies. For these analyses, we performed a reference-based assembly of the RADseq data for the 10 *A. gularis* lineages and *A. costatus* in ipyrad using a reference genome for *A. guttatus* (Barley et al. 2022a). We calculated allele frequencies and blocked  $f_4$ -statistics using the *extract\_f2* function, used the *qpgraph* function to calculate out-of-sample scores for each graph topology, and compared the fit of the 2 best models using bootstrap resampling

(with 100 bootstrap replicates) using the *qpgraph\_resample\_multi* function in the ADMIXTOOLS v2.0.0 R package (Patterson et al. 2012).

### Species Delimitation Inference

A wide variety of approaches have been developed for genetic species delimitation that are conceptually consistent with the general lineage species concept. However, most are agnostic with respect to the mechanism of diversification, which makes it difficult to operationalize them for such purposes. These approaches focus on statistically quantifying levels of genetic divergence and gene flow in different ways. Here, we employ several of these approaches to consider their support for taxonomic hypotheses in which the number of species ranged from 1 to 10 (i.e., the groups of populations showing evidence of genetic differentiation). The genealogical divergence index (*gdi*) quantifies the entire range of potential levels of genetic divergence due to the combined effects of isolation and gene flow, and we used this to quantify the distinctiveness of the 10 lineages. To calculate the posterior distribution of *gdi* values for each lineage, we performed divergence time and population size estimation under the A00 model in BPP v4.3.0 (Leaché et al. 2019). We performed these analyses under 3 alternative topologies to evaluate their effect on estimates of *gdi*: 1) the maximum a posteriori species tree topology from the BPP analysis, 2) the maximum clade credibility tree topology from the concatenated BEAST analysis, and 3) the maximum likelihood topology from the concatenated RaxML analysis. Except for use of the A00 algorithm, we employed the same settings as in the species tree BPP analyses described above. We calculated the *gdi* for each population as  $1 - e^{-2t/\theta}$  using 1000 samples drawn evenly from the posterior distribution. We also ran BPP analyses in which we lumped taxa into 6 and 3 species models, and recalculated *gdi* to evaluate this effect on the estimates. Finally, we used the Hierarchical Heuristic Species Delimitation (HHSD) pipeline to identify a preferred taxonomy based on the *gdi* metric under both the MSC and multispecies coalescent with migration model (MSM) in which bidirectional migration parameters were estimated between geographically adjacent populations (Kornai et al. 2023).

We undertook a series of subsequent analyses to further examine support for the distinctiveness of the 3 primary genetic lineages in the complex. We used Bayes Factors to compare support for 4 tree-based species delimitation models (with 1, 2, or 3 species, including the 2 possible 3-species topologies) to 3 network-based models (with 2 or 3 species) in BPP. For each model, we parameterized the analyses as we did for the *gdi* analyses, except that we performed stepping-stone integration to estimate the marginal likelihood of each model (using 16 power posterior steps, again checking for suitable mixing and that estimates were stable across replicated runs; Flouri et al. 2020). We performed an analysis of fixed genetic differences under the assumption that

if lineages have accumulated fixed allelic differences owing to their genetic isolation, this provides an additional level of support for their evolutionary independence. We used the *dartR* R package (Gruber et al. 2018) to perform the fixed difference analysis after removing individuals with a significant proportion of missing data ( $> 0.4$ ) and admixed ancestry ( $< 0.75$  genetic ancestry from a single group in the STRUCTURE analyses). The goal here was to look for fixed differences that have arisen in the evolutionary history of these lineages while separating out the effect of present day, recent-generation hybrids whose evolutionary contribution may not be significant (Chambers et al. 2023). We included *A. costatus* as an outgroup in these comparisons and assessed if the number of fixed differences was significantly larger than the number expected by chance using 100 simulation replicates. Finally, we used the BA3SNP algorithm in BayesAss (Wilson and Rannala 2003) to estimate rates of recent migration between the 3 lineages, running the analysis for 100 million generations following 5 million generations of burnin, sampling the chain every 10,000 generations, and adjusting the mixing parameters to achieve acceptance rates between 20% and 60% for all parameters.

#### *What Are the Mechanisms of Diversification in Sexual and Unisexual Whiptails?*

After resolving patterns of genetic diversity and evolutionary history within the complex, our final goal was to link these patterns of diversity with mechanisms of diversification. We did this by integrating results from the previous analyses with coalescent modeling, and biogeographic and ecological data. Linking patterns of diversity to evolutionary processes serves 2 purposes: 1) helping to distinguish between interspecific and intraspecific lineages by identifying how these distinctions arose, and 2) providing formal taxonomic/speciation hypotheses that can be further tested using additional data sets. To visualize geographic regions that facilitate and restrict gene flow we used the EEMS (Petkova et al. 2015) software to quantify patterns of nonstationary isolation by distance across the distribution of the *A. gularis* complex. We used the *bed2diffs* program to compute an average genetic dissimilarity matrix for all individuals across all SNPs. We then used this matrix to estimate an effective migration surface for the data set using the *runeems\_snp* program with 500 demes. We ran the analysis for 10 million iterations, following 1 million iterations of burnin, and sampled every 1000 iterations. To identify the context in which divergence and gene flow have occurred between the 3 primary *A. gularis* lineages we compared models of demographic history using the diffusion approximation in *δaδi* (Gutenkunst et al. 2009). We fit 7 coalescent models to the joint allele frequency spectrum that included: 1) strict isolation with no gene flow, 2) divergence with symmetrical gene flow, 3) divergence with asymmetrical gene flow, 4) divergence with asymmetrical gene flow that is heterogeneous across the

genome, 5) secondary contact with symmetrical gene flow, 6) secondary contact with asymmetrical gene flow, and 7) secondary contact with asymmetrical and heterogeneous gene flow (Portik et al. 2017). We used easySFS (<https://github.com/isaacovercast/easySFS>) to identify the down-projected allele sample sizes that maximized the number of segregating sites for each population and randomly sampled a single SNP per locus to estimate the 2-dimensional joint allele frequency spectrum between each pair of populations. We ran a series of optimizations under the Nelder-Mead method to identify the optimal parameter estimates and simulate the joint allele frequency spectrum under each model (see Dryad repository for details). We estimated the likelihood of the spectrum given each model using multinomial optimization and compared models using the Akaike Information Criterion.

To evaluate if niche divergence is associated with genetic variation across populations, we compared ecological niche models (ENMs) between the 3 primary genetic lineages, as the distribution of this complex spans a large geographic range that encompasses significant environmental variation (with populations occurring from sea level up to  $> 2300$  m in elevation). Evidence for ecological differences among lineages that arise from niche modeling is not, by itself, evidence for species distinctiveness. We expect that such difference would be present among almost any populations that span known biogeographical breaks. Rather, these analyses allow us to assess the extent of these differences and may suggest that nascent lineages are more likely to maintain their independence due to processes such as isolation by environment and selection against gene flow, even if they have come back into secondary contact. We constructed niche models using Maxent (Phillips et al. 2017) with the 19 "Bioclim" layers and the elevation data (30 second resolution) available from WorldClim (Fick and Hijmans 2017). We clipped the layers to an extent encompassing the distribution of our population sampling and used default settings in Maxent for the analyses. For distributional data, we downloaded all available records from the Global Biodiversity Information Facility (GBIF) for the taxa *A. gularis* and *A. scalaris* (Downloaded 6/8/21). For each lineage, we created a spatial polygon layer to represent the extent of its distribution based on the results of the genetic analyses. We then removed all nongeoreferenced records from the GBIF data and filtered out points that fell outside the distributional extent for each lineage. Finally, we used R to remove records that had identical locality coordinates, and selected the 500 records that were maximally geographically divergent from all others to reduce spatial autocorrelation for the niche modeling ([github.com/danlwarran/thin.max.R](https://github.com/danlwarran/thin.max.R)). We evaluated model performance in Maxent using the area under the receiver operating characteristic curve (AUC). To compare niche overlap between the Maxent models for each lineage, we calculated Schoener's *D* and Warren's *I* statistics using the *raster.overlap* function in the ENMTools R package (Warren et al. 2021).

To provide further biogeographic context for the *A. gularis* complex, we used a Brownian motion diffusion model to perform ancestral state reconstruction of geographic locations on the phylogenetic history of the group (Quintero et al. 2015). The phylogeny for this analysis was estimated for a single tip for each of the 10 lineages using a concatenated BEAST analysis of the data under the same parameterizations as in the analysis of the larger data set. We also used the estimated evolutionary framework for the *A. gularis* complex as a basis for resolving the hybrid speciation events that produced the 4 unisexual whiptail lineages derived from this group (i.e., identify which gonochoristic lineages are their ancestors). For the diploid unisexual species, we performed a phylogenetic network analysis including the 10 *A. gularis* lineages and the other gonochoristic lineages from which they are thought to be derived by hybridization using PhyloNet. We used the same settings as described in the analyses above that included only the gonochoristic species, except that we set the maximum number of reticulations to 2 (for the 2 unisexual taxa). For the 2 triploid unisexual species, we calculated pairwise  $F_{ST}$  values between each of the *A. gularis* complex lineages and each unisexual lineage using the Weir and Cockerham (1984) method with the snpgdsFst function in the SNPRelate R package (Zheng et al. 2012). We inferred the *A. gularis* lineage with the smallest pairwise  $F_{ST}$  value to be the most likely ancestor of each unisexual. We confirmed that this approach was accurate by checking that the ancestor of the diploids inferred in PhyloNet also had the lowest pairwise  $F_{ST}$  value under this approach.

## RESULTS

### Lineage Diversity in the Spotted Whiptail Lizards

Genetic variation within the *A. gularis* complex is biogeographically structured. There was a large improvement in likelihood score for the  $K = 3$  ( $\ln$  probability of data =  $-109277.3$ ; Fig. 1) versus  $K = 2$  ( $\ln$  probability of data =  $-113895.9$ ; Supplementary Fig. S1) STRUCTURE model, but not for higher values, which also did not show additional geographical structure ( $\ln$  probability of data for  $K = 4$  was  $-109376.1$ ). The 3 primary genetic clusters correspond to 1) populations from the southwestern United States and Northeastern Mexico, 2) populations from the northern Mexican Plateau, and 3) populations from the southern part of the Mexican Plateau (subsequently referred to here as *gularis*, *scalaris*, and *colossus* in shorthand). Individuals from populations near the contact zones between these 3 clusters showed estimates of mixed ancestry from adjacent genetic groups, indicative of the presence of hybrid/admixture zones (Fig. 1). Some of these genetic contact zones are concordant with morphological data from previous studies (Walker 1981b). Under the  $K = 2$  model, the populations from the southern end of the plateau clustered with southwestern United States northern

Mexico populations (Supplementary Fig. S1). The 3 primary clades in the concatenated RAxML analysis of the full data set corresponded to the 3 STRUCTURE genetic clusters and the samples that showed admixed ancestry in STRUCTURE were divergent from other geographically proximate samples, as would be expected in admixed samples whose ancestry is not “tree-like” (Supplementary Fig. S1).

The RAxML analysis also identified substantial genetic structure within the 2 major clades spanning the Mexican Plateau which was concordant with the conStruct analyses. conStruct distinguished as many as 5 genetic groups within the northern and 6 within the southern Mexican Plateau lineage (Supplementary Fig. S2). All of this structure was geographically based and the spatial and nonspatial model results were similar, suggesting much of this was consistent with discrete population structure rather than isolation by distance. We identified 10 lineages based on a synthesis of the population genetic, tree-based genetic diversity, and morphological data to use as a starting point in determining species boundaries (labeled in Fig. 3; Supplementary Appendix 1; Walker 1981a, b). Eight genetic lineages are clearly assignable to taxa described based on morphology (Table 1). The other 2 genetic lineages correspond to populations that had previously been assigned to an undescribed subspecies (Zweifel 1959). One morphologically defined taxon (*semifasciatus*) appears to refer to populations that have mixed ancestry from the 3 primary genetic lineages (discussed further below).

### Patterns of Phylogeny and Gene Flow

The alternative phylogenetic analyses produced discordant topological estimates for the relationships among the 10 *A. gularis* complex lineages (Fig. 4). Most analyses supported the presence of the 3 primary lineages identified in the STRUCTURE analysis, but relationships among them varied across analyses. We suspect this reflects the fact that populations near contact zones between all 3 show evidence of admixture, and thus may have different histories than populations within the 3 lineages that are further from the contact zones. Some analyses identified the primary split in the complex as between *A. gularis* and the remaining populations, whereas others placed *A. gularis* as sister to the populations from the southern Mexican Plateau. The placement of populations from northern Jalisco was also quite variable across analyses. This phylogenetic discordance is likely a consequence of gene flow through introgressive hybridization, as the  $D$ -statistic and  $F$ -branch analyses identified multiple significant introgression tests within the *A. gularis* complex (Fig. 5). The strongest signatures of introgression were between the *semifasciatus* populations and the *rauni* and *gularis* populations. This is consistent with the STRUCTURE analyses which showed that *semifasciatus* populations consisted of genetic ancestry derived from all 3 primary genetic lineages, phylogenetic analysis that recovered

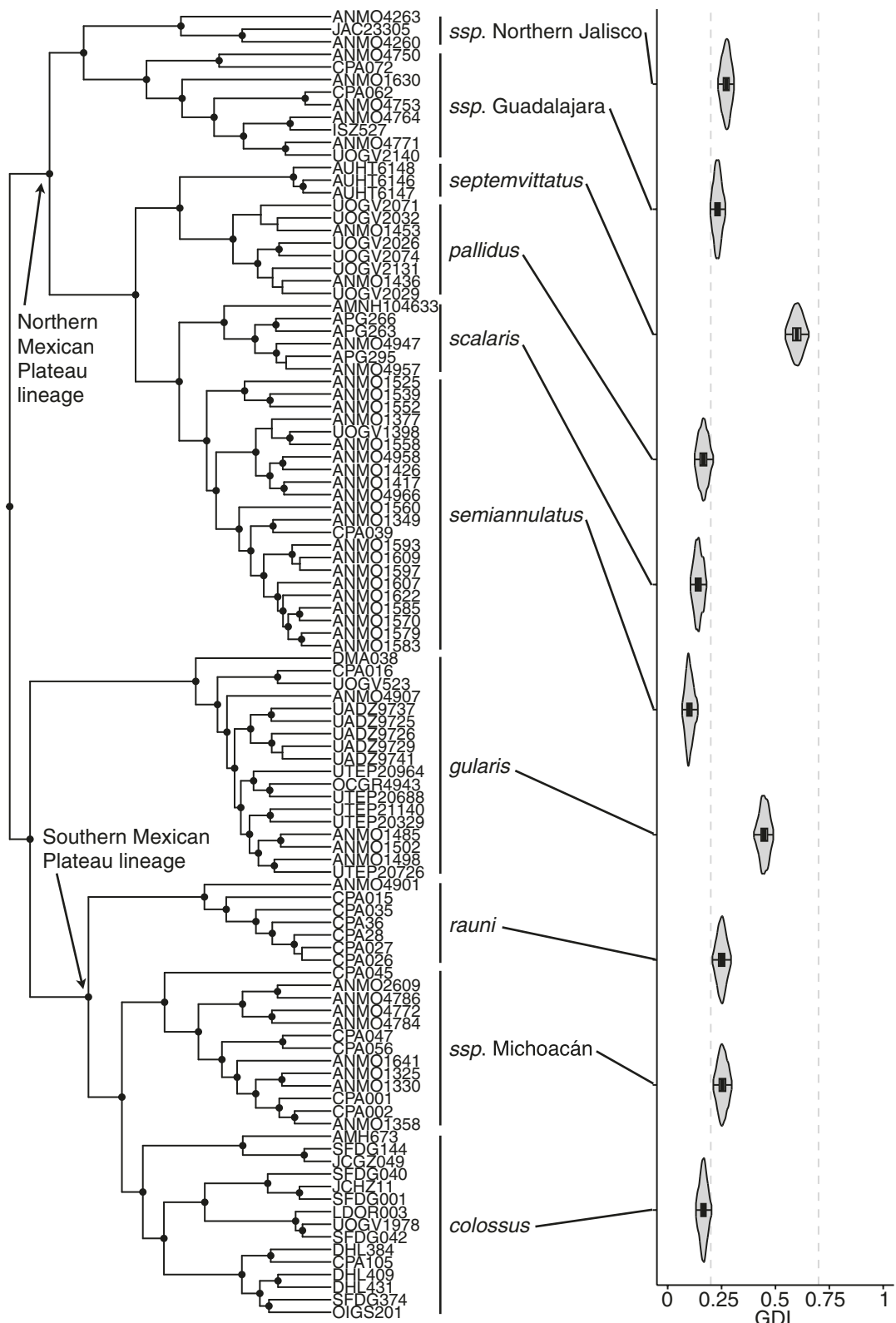


FIGURE 3. Maximum clade credibility chronogram from concatenated BEAST analysis and violin plot of 95% credible interval for genealogical divergence index estimates from BPP under the multispecies coalescent model. Circles at nodes denote those in which the posterior probability  $\geq 0.99$ . Dashed lines indicate proposed thresholds for splitting and lumping lineages as species based on empirical meta-analysis from (Jackson et al. 2017).

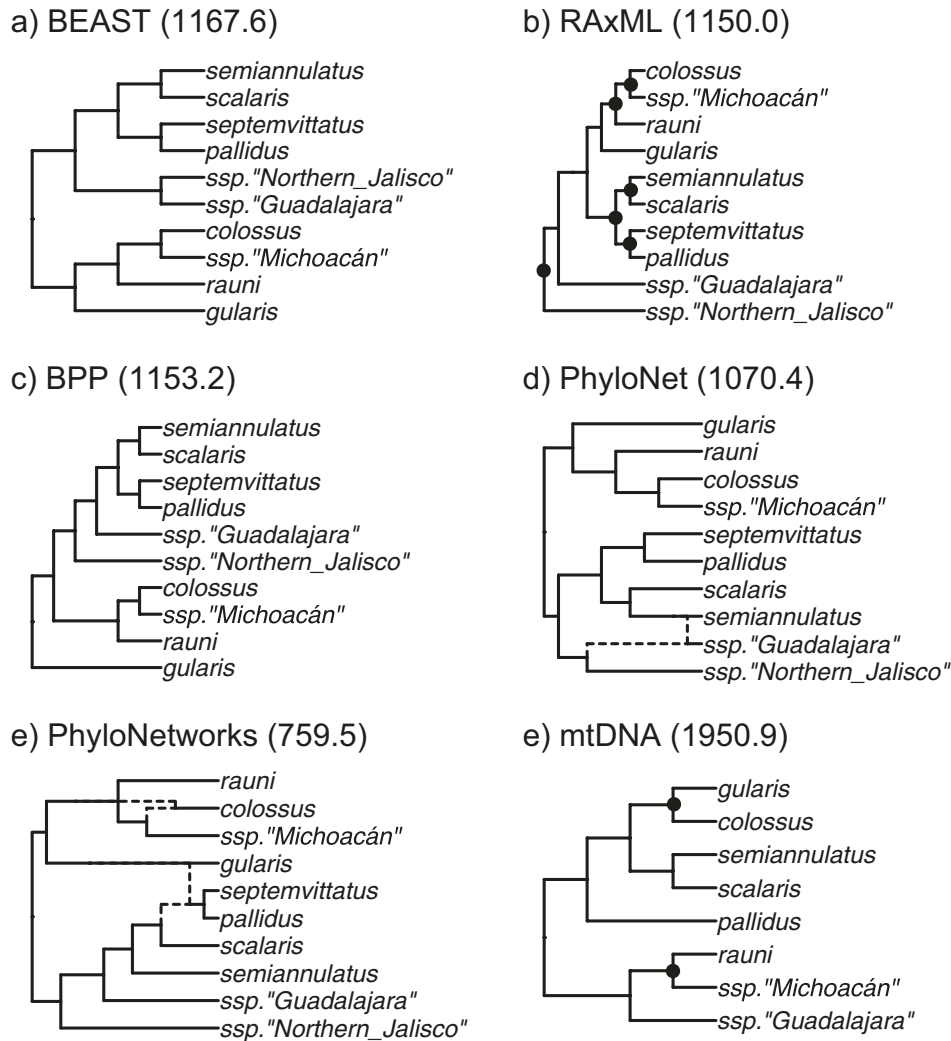


FIGURE 4. Comparison of phylogenetic topologies for 10 spotted whiptail lineages across phylogenetic analyses. Out-of-sample scores from admixture graph comparisons are indicated for each topology. In (a) all nodes in maximum clade credibility tree have posterior probability (pp) = 1.0; in maximum likelihood topologies in (b) and (e), circles at nodes indicate those with bootstrap proportion >0.95; in majority-rule consensus tree in (c) all nodes have pp > 0.95. (d) and (e) show maximum likelihood topologies from the respective analyses.

paraphyly of the geographically cohesive populations, and phylogenetic network analyses demonstrating reticulation at this phylogenetic node (Supplementary Fig. S3). Other signatures of introgression/admixture we detected were between biogeographically adjacent populations and were consistent with previous morphological studies that showed intergradation between these populations (e.g., between *rauni* and both *ssp. Michoacán* and *ssp. Guadalajara*, between *semiannulatus* and *rauni*, between *ssp. Guadalajara* and *semiannulatus*, between *ssp. Michoacán* and *ssp. Guadalajara*, and between *scalaris* and *septemvittatus*).

The PhyloNetworks analysis identified a population tree with 2 reticulations as the optimal network, and these were distinct from the reticulation edge that was inferred in the PhyloNet analysis (exploring models with additional reticulations in the latter analysis was computationally infeasible). The mtDNA gene

tree topology was strikingly divergent from all the RADseq topologies (Fig. 4) and indicated clear signs of admixture/introgression (Supplementary Fig. S4). For example, samples of *rauni* and *ssp. Michoacán* were recovered as members of 2 different clades unlike in the analyses of the RADseq data. Several samples of *pallidus* were also clearly introgressed with *gularis* haplotypes. Finally, one sample of *ssp. Guadalajara* was introgressed with a *semiannulatus* haplotype (the former group of populations was also not monophyletic in the mtDNA gene tree as it was in the RADseq analyses). These instances of discordance due to introgressive hybridization are consistent with biogeographic patterns of distribution between adjacent populations and the *D*-statistic results. Samples of *semifasciatus* also had mtDNA haplotypes that were either derived from *gularis* or *semiannulatus*, which is consistent with the hypothesis that these populations are comprised of

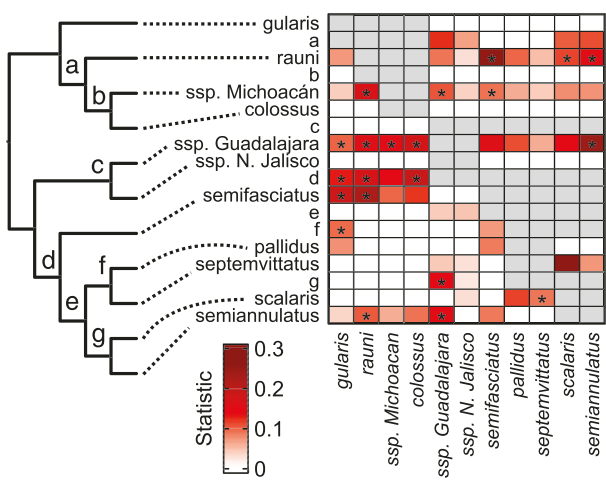


FIGURE 5. F-branch tests for introgression. Assumed topology from BEAST analysis (left). Heatmap illustrating F-branch estimates for each comparison. Darker values indicate larger amounts of discordance that are indicative of introgression, with asterisks denoting statistically significant comparisons with  $Z$  score  $> 8.0$ .

individuals with genomes that are mixtures of multiple genetic lineages (as indicated by the RADseq analyses). The PhyloNetworks topology had the smallest out-of-sample score in the admixture graph comparisons (Fig. 4), which suggested that it was a significantly better fit to the genomic data than the second-best fitting PhyloNet topology ( $p = 2.3e^{-12}$ ;  $z = 7.0$ ). The BEAST analysis topology had the lowest out-of-sample score among the tree-based topologies, although this topology was not a significantly better fit than the RAxML topology ( $P = 0.11$ ,  $z = 1.6$ ).

#### Species Delimitation

Estimated  $gdi$  for the 10 *A. gularis* complex lineages ranged from  $\sim 0.07$  to  $0.65$  (Fig. 3), with mean estimates for each lineage ranging from  $\sim 0.1$  (for *semianulatus* being distinct from *scalaris*) to  $0.6$  (*septemvittatus* being distinct from *pallidus*). The majority of the estimates are within the range of values considered to be ambiguous about the status of a species' distinctiveness (Leaché et al. 2019). The 2 lineages with the highest  $gdi$  values were *gularis* and *septemvittatus*. This likely reflects, in part, the low levels of genetic diversity within these 2 populations and the sensitivity of  $gdi$  estimates to  $\theta$  (i.e., genetic drift occurs more rapidly in smaller populations, causing them to become genetically distinctive, more quickly). Although *gularis* has a relatively large range compared with other lineages in the complex, much of this likely reflects recent, northward postglacial expansion into new habitats in the United States. The assumed topology had little effect on the  $gdi$  estimates (Supplementary Fig. S5). Lumping lineages into 3 and 6 species had minor effects on the  $gdi$  estimates, with *gularis* being identified as the most distinctive taxon under these models (Supplementary Fig. S5). Under the MSC model, the HHSD “split” analysis did not identify

TABLE 2. Results of fixed difference (FD) analyses showing raw number of fixed allelic differences, the number of individuals, and the number of SNPs included in each comparison

	Colossus	Costatus	Gularis
<b>Raw FD</b>			
Costatus	808	—	
Gularis	90	960	
Scalaris	20	807	98
<b>Mean # indiv.</b>			
Costatus	22.9		
Gularis	33.3	17.3	
Scalaris	41.6	25.6	36.0
<b>SNPs</b>			
Costatus	20,740		
Gularis	21,996	20,720	
Scalaris	22,021	20,734	21,994
<b>P-value</b>			
Costatus	0.0000		
Gularis	0.0000	0.0000	
Scalaris	0.9625	0.0000	0.0000

Note:  $P$ -values indicate the significance of each comparison based on 1000 simulation replicates.

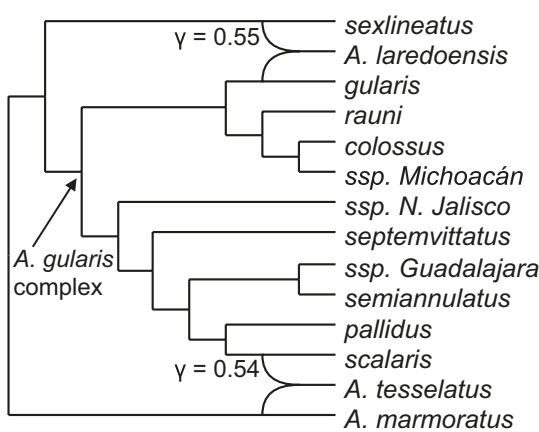
any lineages as distinct when adopting a threshold of 0.7, whereas the “merge” analysis lumped all populations when adopting a threshold of 0.2. Under the MSM model, the “split” analysis results were identical; however, the ‘merge’ analysis identified *gularis*, *rauni*, *colossus*, and *ssp. Michoacán* as distinctive (i.e.,  $gdi > 0.2$ ) and lumped *pallidus*, *septemvittatus*, *scalaris*, *semianulatus*, *ssp. N. Jalisco*, and *ssp. Guadalajara* into a fifth lineage. The fixed difference analysis showed fixed differences between all 3 populations identified by STRUCTURE, but the simulation results suggested that the number of observed differences was not significantly larger than expected by random chance for the *scalaris*–*colossus* comparison (Table 2). The *scalaris*–*colossus* comparison also showed higher estimates for rates of gene flow (whose credible intervals did not include 0) than the comparisons with *gularis* (Supplementary Table S1). The Bayes factor delimitation analyses in BPP suggested there was decisive support for the 3 species tree model in which the *colossus* and *scalaris* lineages were sister taxa over any of the models with fewer species (Table 3).

#### Mechanisms of Diversification

The EEMS analysis inferred lower than average migration rates along the northeastern edge of the Mexican Plateau which generally separates higher elevation populations from lower elevation populations in the complex (Supplementary Fig. S6). It also inferred lower-than-average migration between populations from the southeastern and northwestern parts of the Mexican Plateau, which includes the Trans-Mexican Volcanic Belt, areas that differ in seasonality. Both regions correspond to areas in which the 3 STRUCTURE genetic lineages come into contact, whereas areas of higher-than-average historical migration were inferred among populations within the STRUCTURE genetic clusters. The EEMS analysis also identified 3 regions of lower-than-expected genetic similarity

TABLE 3. Results of Bayes Factor analyses in BPP showing topology of models compared, log marginal likelihood estimates, ranking of models, and Bayes Factors calculated as  $2\ln\text{BF}$

Divergence	N species	MLE	Rank	BF
(outgroup, <i>gularis</i> / <i>scalaris</i> / <i>colossus</i> )	1	-89359.3	7	2586.2
(outgroup, ( <i>gularis</i> , <i>scalaris</i> / <i>colossus</i> ))	2	-89971.9	8	3811.4
(outgroup, ( <i>gularis</i> / <i>colossus</i> , <i>scalaris</i> ))	2	-88529.1	6	925.8
(( <i>gularis</i> , Y) X, ( <i>scalaris</i> / <i>colossus</i> , X) Y, outgroup)	2	-88381.6	4	630.8
(( <i>gularis</i> / <i>colossus</i> , Y) X, ( <i>scalaris</i> , X) Y, outgroup)	2	-88497.1	5	861.8
(outgroup, ( <i>gularis</i> , ( <i>colossus</i> , <i>scalaris</i> )))	3	-88066.2	1	-
(outgroup, ( <i>scalaris</i> , ( <i>colossus</i> , <i>gularis</i> )))	3	-88092.8	3	53.2
(( <i>colossus</i> , ( <i>gularis</i> , Y) X), ( <i>scalaris</i> , X) Y, outgroup)	3	-88076.5	2	20.6



Lineage	<i>exsanguis</i> $F_{ST}$	<i>neotesselatus</i> $F_{ST}$
<i>colossus</i>	0.386	0.427
ssp. <i>Guadalajara</i>	0.329	0.401
<i>gularis</i>	0.438	0.458
ssp. <i>Michoacán</i>	0.413	0.447
ssp. <i>N. Jalisco</i>	0.340	0.413
<i>pallidus</i>	0.335	0.411
<i>rauni</i>	0.397	0.440
<i>scalaris</i>	<b>0.261</b>	<b>0.384</b>
<i>semiannulatus</i>	0.302	0.397
<i>septemvittatus</i>	0.437	0.471

FIGURE 6. Maximum pseudolikelihood network topology illustrating evolutionary history of *A. gularis* complex and diploid unisexual species (*A. laredoensis* & *A. tesselatus*) derived from hybrid speciation involving a parental ancestor for this complex (left).  $\gamma$  represents inheritance probability estimate. Table on right shows pairwise  $F_{ST}$  values between the 2 triploid unisexual species and their potential parental ancestors, with inferred ancestors in bold.

between populations: 1) southwestern Zacatecas and Aguascalientes, 2) the southern end of the Mexican plateau in the state of Mexico, and 3) around the Texas-Mexico border near Big Bend, likely near the location in which *septemvittatus* and *gularis* come into contact. In all cases, the secondary contact coalescent models with asymmetric gene flow fit the allele frequency data better than the continuous gene flow or isolation models (Supplementary Table S2). Model performance was high for all Maxent ENM's (all AUCs > 0.8). There was low niche overlap for all comparisons between the 3 main lineages (Supplementary Fig. S7), although there was higher niche overlap between *scalaris* and *colossus* (Schoener's  $D = 0.1305$ ; Warren's  $I = 0.3321$ ) than either lineage showed with *gularis* (Schoener's  $D = 0.0419$  and Warren's  $I = 0.1274$  for *scalaris* comparison; Schoener's  $D = 0.0225$  and Warren's  $I = 0.0934$  for *colossus* comparison). Variable importance was somewhat divergent across the analyses, although all 3 suggested elevation and temperature seasonality were important (Supplementary Table S3).

The biogeographic reconstructions suggest that the origin of the *A. gularis* complex is in the central region of the Mexican Plateau near northern Zacatecas, and that the present-day distributions of taxa in this group reflect an outward dispersal pattern (Supplementary Fig. S8).

The sister species to the *A. gularis* complex (*A. costatus*) is also known from the extreme southern end of the Mexican Plateau, so this is consistent with the continued northward expansion of this lineage over time. We identified 2 distinctive ancestors that have contributed to the formation of unisexual species: *gularis* as one of the parental ancestors of the diploid unisexual species *A. laredoensis*; and *scalaris* as one of the ancestors of the diploid unisexual *A. tesselatus*, as well as the triploids *A. neotesselatus* and *A. exsanguis* (Fig. 6). This clarifies significant historical confusion about whether these latter 3 taxa are derived from the same ancestral lineage, and if so, which gonochoristic species contributed to their formation (Reeder et al. 2002). For the diploid species, the inferred ancestor was consistent between the phylogenetic network and  $F_{ST}$  approaches.

## DISCUSSION

When species in nascent radiations are related by complex evolutionary histories that include alternating periods of isolation and reticulation, resolving evolutionary history and the boundaries between species can appear intractable. This becomes even more difficult when geographically structured, but confusing, patterns of

genetic and phenotypic variation are present. Here, we developed an approach that integrates phylogenetic and population genetic perspectives to resolve mechanisms of diversification across space and time in the spotted whiptail lizards. The systematics of this complex has historically been considered one of the most difficult taxonomic problems in North America, leading [Duellman and Zweifel \(1962\)](#) to invoke King Lear when finalizing their monographic study of this question “*We realize, however, that our colleagues may come, with Shakespeare, to feel that ‘Tis the times’ plague, when madmen lead the blind’.*” Although generating a stable taxonomy for these lizards may still feel like madness, we are no longer blind to their evolutionary history. Our results suggest that the challenges in understanding the systematics of these lizards result from both present day and historical gene flow among lineages that have diversified morphologically, ecologically, and genetically across complex biogeographic regions. This study also demonstrates the ways in which testing hypotheses related to mechanisms of diversification is an effective means to inform understanding of species boundaries. In this case, 2 lineages diverged allopatrically in distinct environments and despite coming back into secondary contact, have accumulated/maintained fixed genetic and phenotypic differences, contributed differentially to the formation of unisexual species through hybrid speciation, and show low contemporary rates of asymmetrical gene flow at contact zones across ecological gradients. These 2 species each encompass multiple genetic/phenotypic subspecific lineages that show less evidence for contemporary reproductive isolation and evolutionary distinctiveness ([Fig. 2](#)). These results allowed us to clarify the patterns of hybrid speciation that have led to the formation of unisexual whiptail lizards in this group.

#### *Mechanisms of Diversification*

Resolving the systematics of radiations on the speciation continuum is often complicated by the need to understand multiple mechanisms of diversification (e.g., isolation, gene flow) that occur across multiple temporal and geographic scales. These results demonstrate how a pluralistic approach that integrates tools developed for studying different types of evolutionary processes can generate these synthetic insights in complex systems. Biogeographic reconstructions suggest the origin of the *A. gularis* complex to have been in the central Mexican Plateau, followed by subsequent dispersal north and south into geographic regions that vary widely in elevation, habitat, and environment. This has resulted in the differentiation of 10 morphologically and genetically identifiable populations that can be grouped into 3 primary lineages, among which differentiation is much larger. Differentiation among the 3 lineages appears to have been initiated by historical isolation followed by secondary contact, and maintained by selection across environmental gradients that vary in temperature, precipitation, seasonality, and elevation.

Populations at geographically widespread, but narrow, contact zones (i.e., sharp clines in genetic ancestry) show evidence that individuals have ancestry that is significantly admixed among these genetic lineages, but also that rates of gene flow are significantly reduced compared with other parts of the ranges of these lineages. A significant proportion of the genetic differentiation among populations is broadly correlated with phenotypic variation in the form of dorsal coloration. Dorsal phenotypes in these lizards are likely under strong selection pressure due to predation, given their diurnal and highly active foraging behavior, as well as the significant geographic and ontogenetic variation among populations ([Brodie 1989; Stevens and Cuthill 2006; Medina et al. 2017](#)). The presence of light spots on darker, more uniform ground colors versus stripes may be related to conspicuousness in the open versus densely vegetated habitats that these lizards span. However, we do not see an obvious correlation between particular dorsal phenotypes and different habitat types or environments (perhaps with the exception of the uniform-dorsum *pallidus* occurring in a very light substrate habitat). The striking variation in ventral coloration phenotypes across populations is presumably under sexual selection, being more prominent in males and appearing to evolve rapidly.

Biogeographic history also appears to have been important in determining the distribution of unisexual lineages derived from the *A. gularis* complex, of which there are numerous, extant lineages that have formed in the recent past. Their diversification was facilitated by 2 of the northern lineages within the spotted whiptail species complex ([Fig. 6](#)). The gonochoristic *gularis* lineage was the maternal ancestor of the 2 unisexual clones of *A. laredoensis* that were generated by independent primary hybrid speciation events ([Barley et al. 2022b](#)). It appears this lineage invaded the coastal lowlands of northeastern Mexico and Texas through northeastward dispersal from the central Mexican Plateau where it encountered the other gonochoristic parent, *A. sexlineatus*, facilitating the formation of *A. laredoensis* near its present distribution in the Rio Grande River Valley. These data resolve the *scalaris* lineage as the paternal ancestor of the unisexual *A. tesselatus*. That lineage would have dispersed northwestward up the Mexican Plateau, meeting gonochoristic *A. marmoratus* and generating *A. tesselatus* by primary hybrid speciation. *Aspidoscelis tesselatus* later backcrossed with a male *A. sexlineatus* to generate the triploid unisexual species *A. neotesselatus* through hybrid speciation by genome addition (probably even further northward, as this species occurs in southern Colorado). Finally, the *scalaris* lineage was also resolved as the secondary paternal ancestor of *A. exsanguis*, a triploid unisexual species containing genomes from 3 gonochoristic species ([Barley et al. 2022a](#)), derived from an initial hybridization event between 2 distantly related gonochoristic whiptails (*A. burri* and *A. arizonae*), likely in northern Mexico or the southwestern United States. This highly

precise resolution of the ancestry of the unisexual lineages is important to understanding the mechanisms underlying their formation through hybridization. Many attempts to resynthesize unisexual vertebrates that occur in nature through laboratory hybridization of their parental species have been unsuccessful (Cole et al. 2010; Stöck et al. 2010). Part of the reason for this may be that poorly understood genetic factors are important for successful hybrid speciation, and thus in many cases, the unsuccessful attempts may be a consequence of crossing individuals from closely related, but distinct populations from those involved in the historical speciation event. This new understanding opens up opportunities to test this hypothesis and potentially ameliorate challenges to laboratory synthesis of unisexual species.

#### Complex Phylogenetic Histories and Gene Flow

When extensive gene flow occurs between geographically adjacent populations across both contemporaneous and historical timescales, lineages in nascent radiations may have portions of their genome that are derived from multiple ancestral populations. This makes it difficult to reconstruct the historical pattern of evolutionary branching and may cause different statistical methods (each with varying simplifying assumptions) to produce strongly supported, discordant topologies, as we observed in this study. We employed several approaches to deal with this issue: 1) analyzing the data with a variety of phylogenetic and population genetic tools that vary in their assumptions with respect to horizontal gene transfer, 2) removing individuals from analyses that come from hybrid zones and appear to be recent generation hybrids whose individual genetic history obscures the deeper evolutionary history that we are attempting to study, and then 3) modeling reticulate evolution directly ( $D$ -statistics and phylogenetic networks). This approach identified the *semifasciatus* populations from southeastern Coahuila as having a manifold hybrid background (Figs. 1 and 5 Supplementary Fig. S3) and populations in other areas on the eastern edge of the Mexican Plateau as having relatively equal estimates of genetic ancestry from 2 primary groups (perhaps indicative of F1 or F2 hybrid individuals). These occur in San Luis Potosi, Nuevo Leon, and near Cuatro Ciénegas, Coahuila, with the latter corresponding to a population that also shows a hybrid morphology (Walker et al. 1981b).

Results of this study also highlight how horizontal genetic exchange between lineages where they come into contact may cause the relationships among them to vary in different parts of their ranges and contribute to phylogenetic discordance. For example, phylogenetic analyses show the *gularis* lineage either being placed as sister to the rest of the complex, or as more closely related to the populations from the southern end of the Mexican Plateau. Another challenge involves populations from the southwestern edge of the Mexican Plateau in northern Jalisco, which either appear to be

sister to all other populations in the complex or related to several other populations near the Trans-Mexican Volcanic Belt. Broader studies of the *A. sexlineatus* species group (within which the *gularis* complex is placed) have found evidence for introgression between *A. gularis* complex lizards and closely related outgroup taxa (*A. occidentalis*; Barley et al. 2022a). *Aspidoscelis occidentalis* potentially contacts *scalaris* populations in Nayarit and Jalisco, so historical hybridization between them is a plausible hypothesis. The  $K = 3$  STRUCTURE model also inferred a small proportion of ancestry in these northern Jalisco populations as being drawn from *gularis*, despite the large distance separating them, and we suspect it is these introgressed regions that the model is picking up on (Fig. 1). Alternatively, this genetic ancestry may reflect an instance of ancient ghost introgression from an extinct population that gave rise to the *A. gularis* complex, which may be an important source of phylogenetic discordance in lineages in which hybridization is common (Ottenburghs 2020; Tricou et al. 2022). Given the seemingly ubiquitous nature of gene flow in the *A. gularis* complex, all the evolutionary networks we inferred are likely a somewhat simplified estimate of the history of these lineages. However, using this integrative approach, we were able to distinguish aspects of evolutionary history that are largely tree-like and highlight the strongest signatures of introgression/admixture in the data set.

#### Species Delimitation and Taxonomy

One of the most striking patterns across the tree of life is the variation in the rate at which morphological and genetic variation accumulate in populations (Dobzhansky 1937; Mayr 1942; Rundell and Price 2009). In combination with the fact that speciation often appears to be a largely continuous process, this challenges systematists (especially those with different working conceptions of species) to identify robust taxonomies. North American whiptail lizards are an extreme example of the rapid evolution of ubiquitous geographic variation, and our results demonstrate how this challenge is present even when the demographic histories of lineages are well-understood. More than 75 North American whiptail lizard taxa have been described based on morphology, many of whose status as species or subspecies has changed over time (Wright 1993). This rapid evolution of phenotypes is challenging to interpret because morphological differentiation may then not be a good proxy for the likelihood that speciation has occurred (Hillis et al. 2021). Within the *A. gularis* complex, coloration phenotypes exhibit striking variation (Walker et al. 1981a,b): the dorsal phenotypes of adult lizards in this group range from an alternating series of light and dark stripes interspersed with faint spots, to a series of lateral bars or large spots, to nearly unicolor, or containing numerous small, distinct spots. Throat and chest coloration in these lizards is also highly variable across populations, with colors encompassing black, blue, red, orange, or white in adult

males. This variation has led to the description of 8 taxa; however, many areas of phenotypic intergradation occur between these populations (phenotypic variation in this group is correlated with genetic variation, but not always in a straightforward manner). Here we focus on genomic insights into the nature of species boundaries and consider how, even when the demographic history of a complex is well-resolved, taxonomists may arrive at different conclusions about them (see the **Supplementary materials** for a detailed discussion of historical taxonomy in the group).

Although we suspect the majority of the 10 *A. gularis* lineages are subspecific in nature, it is informative to consider how taxonomists with more liberal operational perspectives on the general lineage concept of species might disagree. For example, some authors have suggested that if there are differences in genetics and morphology, one should give a name to even the most fine-scale divisions at the tips of the tree of life (Torstrom et al. 2014; Burbrink and Ruane 2021; Burbrink et al. 2022). In addition to philosophical objections to this view, there are methodological challenges to implementing this approach. For example, admixed populations can be misinterpreted to be highly divergent phylogenetic clades when researchers employ tree-based approaches to genetic species delimitation (Chan et al. 2021). We see some evidence of this within the spotted whiptails in both the admixed *semifasciatus* populations in Coahuila and the northern Jalisco populations. Coalescent methods are less sensitive to this issue, but can also be subject to bias due to model misspecification and the propensity to conflate population splits with speciation (Jackson et al. 2017; Barley et al. 2018; Leaché et al. 2019). The genealogical divergence index has been proposed to more accurately characterize uncertainty in measures of population distinctiveness, but our study illustrates some challenges with this approach. *gdi* estimates are highly dependent on estimates of  $\theta$  (we see the largest values within lineages that have limited genetic variability; **Supplementary Fig. S5**) and this metric is sometimes discordant with respect to species status between sister lineages that have differing levels of intraspecific genetic variation. This is further complicated by the fact that *gdi* estimates are dependent on the assumed phylogenetic model and that the choice of threshold for splitting or lumping taxa will have a strong impact on the conclusion. Given the diversity of speciation processes that occur across systems, comparison of the *gdi* metric between clades in which species boundaries are understood and those in which they are not as a means of making taxonomic decisions is not always straightforward. This is particularly true among lineages on the 'speciation continuum', where *gdi* estimates may often fall within a range of values observed at both intraspecific and interspecific levels, as we see here. Results from this study also suggest that use of the multispecies-coalescent-with-introgression model (vs. the MSC) does not alleviate challenges to using Bayesian model selection to delimit

species. Bayes Factors analyses under tree and network models of speciation still showed extremely decisive support for each of these 3 lineages as distinct (Ln Bayes Factor  $>> 5$ ) despite their ambiguous *gdi* values under the heuristic approach.

Because gene flow occurs between even the most divergent lineages in the *A. gularis* complex, more conservative taxonomists that regard complete reproductive isolation as the paramount criterion for species recognition might argue that the entire complex be regarded as a single polytypic species (Walker et al. 1981a; Hillis et al. 2021; Dufresnes et al. 2023). We view this as perhaps too severe a threshold. Two primary parameters are important in determining the likelihood of speciation during lineage divergence: divergence time and rate of gene flow. Based on the credible interval estimate of  $\tau$  from the best BPP delimitation model (**Table 3**) and an assumed typical vertebrate mutation rate of  $1 \times 10^{-8}$ , the divergence time estimates for all 3 lineages exceed 100,000 years, a reasonable estimate of time for parapatric speciation to occur (Gavrilets 2000). That being said, the credible intervals for our estimates of recent migration rates between them encompass values that might be considered high if speciation has occurred (e.g.,  $m \geq 0.1$ ; **Supplementary Table S1**). Given the significant genetic, morphological, and ecological differentiation between the *gularis* lineage and the remaining populations in the complex, a strong case can be made to recognize that lineage at the species level despite secondary contact accompanied by some limited gene flow at contact zones. A 2 species arrangement for the complex has been followed by recent authors (The Reptile Database; <http://www.reptile-database.org>), so a taxonomic stability argument for the continued recognition of 2 lineages pending subsequent evidence could also be applied. Results of this study further suggest the distinction between the 2 lineages is biologically important because they have given rise to different unisexual whiptail lineages through hybrid speciation with alternative gonochoristic partners (**Fig. 6**). Given the uncertainty in how the *gularis* lineage is related to the remaining populations, it is not completely clear which of the 2 lineages should be assigned which subspecies, although we provide a recommendation here that is consistent with previous taxonomic work (**Fig. 2**; Walker et al. 2001).

Populations from the southern end of the Mexican Plateau also appear to exhibit significant genetic, ecological, and morphological differentiation from those from the north. Although there are broad zones of contact between all 3 primary lineages, they are associated with turnover in patterns in genetic ancestry over relatively short geographic distances. Coalescent modeling also suggests that rates of gene flow between lineages is asymmetric and heterogeneous across the genome, which is consistent with some reproductive isolation among them. Given this, we suspect that some taxonomists would argue for a 3 species arrangement, but we refrain from elevating this group of populations here

pending further clarity and a wish to avoid introducing further taxonomic confusion. Interestingly, reviewers of this manuscript were split in terms of their preference for a 1 species or 3 species solution, reflecting how philosophical differences among taxonomists may arise even when they operate under similar species concepts.

These challenges highlight the multiple benefits of making taxonomic decisions within the context of specific hypotheses or models that mechanistically describe how speciation likely occurred. For one, this directly connects taxonomy to the evolutionary processes that generate diversity (e.g., as opposed to statistical thresholds that can at times be divorced from biology). It also reduces scientific dependence on taxonomic authority, allowing individual researchers to make evidence-based decisions about alternative taxonomies, based on explicit methodological or philosophical grounds. Finally, this approach provides methodological guidance for resolving taxonomic ambiguities and facilitates the development of criteria for resolving disputes. For example, hybrid zones between *A. gularis* and *A. scalaris* could be studied at multiple locations (such as west of Cuatro Ciénegas, Coahuila, and north of Big Bend, TX) to determine if intrinsic reproductive isolation occurs between populations in both regions (confirming their species status; Chambers et al. 2023). Additional intriguing patterns of genetic and morphological variation are also present among populations in the complex whose biological nature is not clear. In these cases, contact zone transects could be studied to demonstrate a lack of clinal variation and barriers to gene flow (e.g., populations on the southern end of the Mexican Plateau in Jalisco). Ideally, these could be paired with ecological studies of phenotypically distinct populations to identify if any of the striking morphological variation is under natural or sexual selection (Brodie 1992; Kwiatkowski and Sullivan 2002). Subsequently, genome association studies to identify the genomic basis of any adaptive genetic variation or Dobzhansky–Muller incompatibilities would serve to validate speciation hypotheses (Hoekstra et al. 2006; Schumer et al. 2014; Long and Rieseberg 2024).

#### Concluding Remarks

In this study, we integrate genomic data sets with a range of models to illustrate the practical and philosophical challenges that widespread gene flow and hybridization pose to understanding phylogenetic history and species boundaries. Results of this work demonstrate how adoption of an evolutionary process-focused framework can facilitate systematic progress in the face of these challenges, and generate insights into the evolutionary diversity of a group of vertebrates that have plagued systematic biologists for over a century. The ubiquity of genetic and phenotypic divergence and gene flow between populations of these lizards will allow it to serve as a model for understanding complex processes that are often present to a lesser degree in other systems along the speciation continuum.

#### SUPPLEMENTARY MATERIAL

Data available from the Dryad Digital Repository: <https://dx.doi.org/10.5061/dryad.wwpzgmss1>.

#### ACKNOWLEDGMENTS

We thank the University of Texas El Paso Biodiversity Collections, the American Museum of Natural History, Randy Klabacka, and the Auburn University Museum of Natural History for providing tissue samples for this research. We also thank Uri García-Vázquez, Israel Solano-Zavaleta, Lauren Livo, and A. Peralta for providing tissue samples for this study. We thank Daniel Lara-Tufiño, Max Monroy, and Anahí Esquivel-Ramírez for assistance with fieldwork. We thank James Walker for valuable discussions about the biology and systematics of *Aspidoscelis* lizards. We thank the Secretaría de Medio Ambiente y Recursos Naturales, Dirección General de Vida Silvestre for providing sampling permits for this research. We thank Shana McDevitt at the Vincent J. Coates Genomics Sequencing Lab at U. C. Berkeley and Graham Wiley at the Oklahoma Medical Research Foundation for assistance with the Illumina sequencing. We used computational resources provided by Arizona State University Research Computing and University of Hawaii Information Technology Services for performing some of the analyses in our study. Financial support was provided by grants from the Arnold and Mabel Beckman Foundation, the National Science Foundation Division of Environmental Biology (DEB-1754350 and DEB-190017) and Programa de Apoyo a Proyectos de Investigación e Innovación Tecnológica, Universidad Nacional Autónoma de México (no. IN218522). We thank Gary Nafis, Emmanuel Guevara Lazcano, Luis Stevens, and Leonor Vázquez Rivera for providing excellent photos for illustrating some of the phenotypic variation in these lizards.

#### DATA AVAILABILITY

Raw genomic sequence data used in this research are available at NCBI BioProject SRA PRJNA707030, PRJNA762930, PRJNA827355, PRJNA1016487, and PRJNA1134690.

#### REFERENCES

- Avise, J.C. 2008. *Clonality: the genetics, ecology, and evolution of sexual abstinence in vertebrate animals*. Oxford: Oxford University Press.
- Baird S.F., Girard C.F. 1852. Characteristics of some new reptiles in the Museum of the Smithsonian Institution, part 2. *Proc. Acad. Nat. Sci. Phil.* 6:125–129.
- Barley A.J., Brown J.M., Thomson R.C. 2018. Impact of model violations on the inference of species boundaries under the multispecies coalescent. *Syst. Biol.* 67:269–284.

Barley A.J., Cordes J.E., Walker J.M., Thomson R.C. 2022b. Genetic diversity and the origins of parthenogenesis in the teiid lizard *Aspidoscelis laredoensis*. *Mol. Ecol.* 31:266–278.

Barley A.J., de Oca A.N.M., Manríquez-Morán N.L., Thomson R.C. 2022a. The evolutionary network of whiptail lizards reveals predictable outcomes of hybridization. *Science*. 377:773–777.

Barley A.J., Nieto-Montes de Oca A., Reeder T.W., Manríquez-Morán N.L., Arenas Monroy J.C., Hernández-Gallegos O., Thomson R.C. 2019. Complex patterns of hybridization and introgression across evolutionary timescales in Mexican whiptail lizards (*Aspidoscelis*). *Mol. Phylogenet. Evol.* 132:284–295.

Barley A.J., Reeder T.W., de Oca A.N.M., Cole C.J., Thomson R.C. 2021. A new diploid parthenogenetic whiptail lizard from Sonora, Mexico, is the “missing link” in the evolutionary transition to polyploidy. *Am. Nat.* 198:295–309.

Bouckaert R., Heled J., Kühnert D., Vaughan T., Wu C.-H., Xie D., Drummond A., Rambaut A., Drummond A.J. 2014. BEAST 2: a software platform for Bayesian evolutionary analysis. *PLoS Comput. Biol.* 10:e1003537.

Brabuord G.S., Coop G.M., Ralph P.L. 2018. Inferring continuous and discrete population genetic structure across space. *Genetics*. 210:33–52.

Brodie E.D. 1989. Genetic correlations between morphology and antipredator behaviour in natural populations of the garter snake *Thamnophis ordinoides*. *Nature*. 342:542–543.

Brodie E.D. 1992. Correlational Selection for Color Pattern and Antipredator Behavior in the Garter Snake *Thamnophis ordinoides*. *Evolution*. 46:1284–1298.

Burbrink F.T., Crother B.I., Murray C.M., Smith B.T., Ruane S., Myers E.A., Pyron R.A. 2022. Empirical and philosophical problems with the subspecies rank. *Ecol. Evol.* 12:e9069.

Burbrink F.T., Ruane S. 2021. Contemporary philosophy and methods for studying speciation and delimiting species. *Ichthyol Herpetol.* 109:874–894.

Campillo L.C., Barley A.J., Thomson R.C. 2020. Model-based species delimitation: are coalescent species reproductively isolated? *Syst. Biol.* 69:708–721.

Carstens B.C., Pelletier T.A., Reid N.M., Satler J.D. 2013. How to fail at species delimitation. *Mol. Ecol.* 22(17):4369–4383.

Chambers E.A., Marshall T.L., Hillis D.M. 2023. The importance of contact zones for distinguishing interspecific from intraspecific geographic variation. *Syst. Biol.* 72:357–371.

Chan K.O., Hutter C.R., Wood P.L., Su Y.-C., Brown R.M. 2021. Gene flow increases phylogenetic structure and inflates cryptic species estimations: a case study on widespread Philippine puddle frogs (*Occidozyga laevis*). *Syst. Biol.* 71:40–57.

Cole C.J., Hardy L.M., Dessauer H.C., Taylor H.L., Townsend C.R. 2010. Laboratory hybridization among North American whiptail lizards, including *Aspidoscelis tigris marmorata* (Squamata, Teiidae), ancestors of unisexual clones in nature. *Am. Mus. Novit.* 3698:1–43.

Cope E.D. 1892. A synopsis of the species of the teiid genus *Cnemidophorus*. *Trans. Am. Phil. Soc.* 17:27–52.

Cope E.D. 1900. Crocodilians, lizards, and snakes of North America. Annual Report of the U.S. National Museum for 1898. Washington D.C.: The United States National Museum: 151–1294.

de Queiroz, K. 1998. The general lineage concept of species, species criteria, and the process of speciation: a conceptual unification and terminological recommendations. In: Howard D. J., Berlocher S. H., editors. *Endless Forms: Species and Speciation*. Oxford: Oxford University Press. p. 57–75

De Queiroz K. 2007. Species concepts and species delimitation. *Syst. Biol.* 56:879–886.

Dixon J.R., Lieb C.S., Ketchersid C.A. 1971. A new lizard of the genus *Cnemidophorus* (Teiidae) from Queretaro, Mexico. *Herpetologica*. 27:344–354.

Dobzhansky, T. (1937). *Genetics and the origin of species*. New York: Columbia University Press.

Duellman W.E., Zweifel R.G. 1962. A synopsis of the lizards of the *sexlineatus* group (genus *Cnemidophorus*). *Bull. Am. Mus. Nat. Hist.* 123:155–210.

Dufresnes C., Poyarkov N., Jablonski D. 2023. Acknowledging more biodiversity without more species. *Proc. Natl. Acad. Sci. U.S.A.* 120:e2302424120.

Dufresnes C., Pribille M., Alard B., Gonçalves H., Amat F., Crochet P.A., Martínez-Solano I., Perrin N., Fumagalli L., Vences M., Martínez-Solano I. 2020. Integrating hybrid zone analyses in species delimitation: lessons from two anuran radiations of the Western Mediterranean. *Heredity*. 124:423–438.

Eaton D.A.R., Overcast I. 2020. ipyRAD: interactive assembly and analysis of RADseq datasets. *Bioinformatics*. 36:2592–2594.

Edgar R.C. 2004. MUSCLE: multiple sequence alignment with high accuracy and high throughput. *Nucleic Acids Res.* 32:1792–1797.

Esquivel-Ramírez A., Hornung-Leoni C.T., Manríquez-Morán N.L. 2021. Morphological variation and sexual dimorphism in the *Aspidoscelis gularis* complex (Squamata: Teiidae) from Mexico. *Acta Zool.* 102(2):129–142.

Fick S.E., Hijmans R.J. 2017. WorldClim 2: new 1-km spatial resolution climate surfaces for global land areas. *Int. J. Climatol.* 37:4302–4315.

Flouri T., Jiao X., Rannala B., Yang Z. 2020. A Bayesian implementation of the multispecies coalescent model with introgression for phylogenomic analysis. *Mol. Biol. Evol.* 37:1211–1223.

Gadow H. 1906. A contribution to the study of evolution based upon the Mexican species of *Cnemidophorus*. *Proc. Zool. Soc. Lond.* 76:277–375.

Galtier N. 2019. Delineating species in the speciation continuum: a proposal. *Evol. Appl.* 12:657–663.

Gavrilets S. 2000. Waiting time to parapatric speciation. *Proc. Biol. Sci.* 267:2483–2492.

Gruber B., Unmack P.J., Berry O.F., Georges A. 2018. dartr: an R package to facilitate analysis of SNP data generated from reduced representation genome sequencing. *Mol. Ecol. Resour.* 18:691–699.

Gutenkunst R.N., Hernandez R.D., Williamson S.H., Bustamante C.D. 2009. Inferring the joint demographic history of multiple populations from multidimensional SNP frequency data. *PLoS Genet.* 5:e1000695.

Hartop E., Srivathsan A., Ronquist F., Meier R. 2022. Towards large-scale integrative taxonomy (LIT): resolving the data conundrum for dark taxa. *Syst. Biol.* 71(6):1404–1422.

Hibbins M.S., Hahn M.W. 2022. Phylogenomic approaches to detecting and characterizing introgression. *Genetics*. 220:iyab173.

Hillis D.M., Chambers E.A., Devitt T.J. 2021. Contemporary methods and evidence for species delimitation. *Ichthyol Herpetol.* 109:895–903.

Hoekstra H.E., Hirschmann R.J., Bunde R.A., Insel P.A., Crossland J.P. 2006. A single amino acid mutation contributes to adaptive beach mouse color pattern. *Science* 313:101–104.

Jackson N.D., Carstens B.C., Morales A.E., O’Meara B.C. 2017. Species delimitation with gene flow. *Syst. Biol.* 66:799–812.

Kornai D., Flouri T., Yang Z. 2023. Hierarchical heuristic species delimitation under the multispecies coalescent model with migration. *BioRxiv*. doi: [10.1101/2023.09.10.557025](https://doi.org/10.1101/2023.09.10.557025)

Kwiatkowski M.A., Sullivan B.K. 2002. Geographic variation in sexual selection among populations of an iguanid lizard, *Sauromalus obesus* (=ater). *Evolution*. 56(10):2039–2051.

Leaché A.D., Harris R.B., Rannala B., Yang Z. 2014. The influence of gene flow on species tree estimation: a simulation study. *Syst. Biol.* 63:17–30.

Leaché A.D., Zhu T., Rannala B., Yang Z. 2019. The spectre of too many species. *Syst. Biol.* 68:168–181.

Long Z., Rieseberg L.H. 2024. Documenting homoploid hybrid speciation. *Mol. Ecol.*: e17412. doi: <https://doi.org/10.1111/mec.17412>

Malinsky M., Matschiner M., Svardal H. 2021. Dsuite - Fast D -statistics and related admixture evidence from VCF files. *Mol. Ecol. Resour.* 21:584–595.

Mayr E. 1942. *Systematics and the Origin of Species from the Viewpoint of a Zoologist*. New York: Columbia University Press.

McLean C.A., Stuart-Fox D. 2014. Geographic variation in animal colour polymorphisms and its role in speciation. *Biol. Rev. Camb. Philos. Soc.* 89:860–873.

Medina I., Losos J.B., Mahler D.L. 2017. Evolution of dorsal pattern variation in Greater Antillean *Anolis* lizards. *Biol. J. Linn. Soc.* 120:427–435.

Miller, M.A., Pfeiffer, W., and Schwartz, T. (2010) “Creating the CIPRES Science Gateway for inference of large phylogenetic trees” in Proceedings of the Gateway Computing Environments Workshop (GCE), 14 Nov. 2010, New Orleans, LA. pp. 1–8.

Mirarab S., Nakhleh L., Warnow T. 2021. Multispecies coalescent: theory and applications in phylogenetics. *Annu. Rev. Ecol. Evol. Syst.* 52:247–268.

Moritz C., Brown W.M., Densmore L.D., Wright J.W., Vyas D., Donellan S., ... Baverstock P. 1989. Genetic diversity and the dynamics of hybrid parthenogenesis in *Cnemidophorus* (Teiidae) and *Heteronotia* (Gekkonidae). In *Evolution and ecology of unisexual vertebrates*. New York: The University of State of New York. p. 87–112.

Olave M., Meyer A. 2020. Implementing large genomic single nucleotide polymorphism data sets in phylogenetic network reconstructions: a case study of particularly rapid radiations of cichlid fish. *Syst. Biol.* 69:848–862.

Ottenburghs J. 2020. Ghost introgression: Spooky gene flow in the distant past. *Bioessays*. 42:2000012.

Pang X.-X., Zhang D.-Y. 2024. STRUCTURE and hybridization detection: a cautionary note on using STRUCTURE to detect hybridization in a phylogenetic context. *BioRxiv*. doi: [10.1101/2024.02.06.579057](https://doi.org/10.1101/2024.02.06.579057)

Patterson N., Moorjani P., Luo Y., Mallick S., Rohland N., Zhan Y., Reich D., Webster T., Reich D. 2012. Ancient admixture in human history. *Genetics*. 192:1065–1093.

Pavón-Vázquez C.J., Rana Q., Farleigh K., Crispo E., Zeng M., Liliyah J., Blair C., Ascanio A., Jezkova T., Leaché A.D., Flouri T., Yang Z., Blair C. 2024. Gene flow and isolation in the arid Nearctic revealed by genomic analyses of desert spiny lizards. *Syst. Biol.* 73:323–342.

Peterson B.K., Weber J.N., Kay E.H., Fisher H.S., Hoekstra H.E. 2012. Double digest RADseq: an inexpensive method for de novo SNP discovery and genotyping in model and non-model species. *PLoS One* 7:e37135.

Petkova D., Novembre J., Stephens M. 2015. Visualizing spatial population structure with estimated effective migration surfaces. *Nat. Genet.* 48:94–100.

Phillips S.J., Anderson R.P., Dudík M., Schapire R.E., Blair M.E. 2017. Opening the black box: an open-source release of Maxent. *Ecography*. 40:887–893.

Portik D.M., Leaché A.D., Rivera D., Barej M.F., Burger M., Hirschfeld M., Fujita M.K., Blackburn D.C., Fujita M.K. 2017. Evaluating mechanisms of diversification in a Guineo-Congolian tropical forest frog using demographic model selection. *Mol. Ecol.* 26:5245–5263.

Pritchard J.K., Stephens M., Donnelly P. 2000. Inference of population structure using multilocus genotype data. *Genetics*. 155:945–959.

Puritz J.B., Hollenbeck C.M., Gold J.R. 2014. dDocent: A RADseq variant-calling pipeline designed for population genomics of non-model organisms. *PeerJ* 2:e431.

Pyron R.A., O'Connell K.A., Duncan S.C., Burbrink F.T., Beamer D.A. 2023. Speciation hypotheses from phylogeographic delimitation yield an integrative taxonomy for seal salamanders (*Desmognathus monticola*). *Syst. Biol.* 72:179–197.

Quintero I., Keil P., Jetz W., Crawford F.W. 2015. Historical biogeography using species geographical ranges. *Syst. Biol.* 64:1059–1073.

Rambaut A., Drummond A.J., Xie D., Baele G., Suchard M.A. 2018. Posterior summarization in Bayesian phylogenetics using Tracer 1.7. *Syst. Biol.* 67:901–904.

Ramírez-Portilla C., Quattrini A.M. 2023. Perspectives on the grey zone of species delimitation with notes on invertebrates in the marine environment. *Bull. Soc. Syst. Biol.* 2:1–23.

Rannala B., Yang Z. 2017. Efficient Bayesian species tree inference under the multispecies coalescent. *Syst. Biol.* 66:823–842.

Reeder T.W., Cole C.J., Dessauer H.C. 2002. Phylogenetic relationships of whiptail lizards of the genus *Cnemidophorus* (Squamata: Teiidae): a test of monophyly, reevaluation of karyotypic evolution, and review of hybrid origins. *Am. Mus. Novit.* 3365:1–61.

Rundell R.J., Price T.D. 2009. Adaptive radiation, nonadaptive radiation, ecological speciation and nonecological speciation. *Trends Ecol. Evol.* 24(7):394–399.

Schumer M., Cui R., Powell D.L., Dresner R., Rosenthal G.G., Andolfatto P. 2014. High-resolution mapping reveals hundreds of genetic incompatibilities in hybridizing fish species. *ELife* 3:1–21.

Shaw K.L., Mullen S.P. 2014. Speciation continuum. *J. Hered.* 105:741–742.

Smith M.L., Carstens B.C. 2020. Process-based species delimitation leads to identification of more biologically relevant species. *Evolution*. 74:216–229.

Solís-Lemus C., Ané C. 2016. Inferring phylogenetic networks with maximum pseudolikelihood under incomplete lineage sorting. *PLoS Genet.* 12:e1005896.

Stamatakis A. 2014. RAxML version 8: a tool for phylogenetic analysis and post-analysis of large phylogenies. *Bioinformatics*. 30:1312–1313.

Stevens M., Cuthill I.C. 2006. Disruptive coloration, crypsis and edge detection in early visual processing. *Proc. Biol. Sci.* 273:2141–2147.

Stöck M., Lampert K.P., Möller D., Schlupp I., Schartl M. 2010. Monophyletic origin of multiple clonal lineages in an asexual fish (*Poecilia formosa*). *Mol. Ecol.* 19:5204–5215.

Torstrom S.M., Pangle K.L., Swanson B.J. 2014. Shedding subspecies: the influence of genetics on reptile subspecies taxonomy. *Mol. Phylogenet. Evol.* 76:134–143.

Tricou T., Tannier E., de Vienne D.M. 2022. Ghost lineages highly influence the interpretation of introgression tests. *Syst. Biol.* 71:1147–1158.

Walker J.M. 1966. Morphological variation in the Teiid lizard *Cnemidophorus gularis*. Ph.D. thesis, University of Colorado.

Walker J.M. 1981a. Systematics of *Cnemidophorus gularis*. I. Reallocation of populations currently allocated to *Cnemidophorus gularis* and *Cnemidophorus scalaris* in Coahuila, México. *Copeia*. 1981:826–849.

Walker J.M. 1981b. Systematics of *Cnemidophorus gularis*. II. Specific and subspecific identity of the Zacatecas Whiptail (*Cnemidophorus gularis semiannulatus*). *Copeia*. 1981:850–868.

Walker J.M., Lemos-Espinal J.A., Cordes J.E., Taylor H.L., Smith H.M. 2001. Allocation of populations of whiptail lizards to *septemvittatus* Cope, 1892 (genus *Cnemidophorus*) in Chihuahua, México, and the *scalaris* problem. *Copeia*. 2001:747–765.

Warren D.L., Matzke N.J., Cardillo M., Baumgartner J.B., Beaumont L.J., Turelli M., Dinnage R., Huron N.A., Simões M., Iglesias T.L., Piquet J.C., Dinnage R. 2021. ENMTools 1.0: an R package for comparative ecological biogeography. *Ecography*. 44(4):504–511.

Weir B.S., Cockerham C.C. 1984. Estimating F-statistics for the analysis of population structure. *Evolution*. 38(6):1358–1370.

Wilson G.A., Rannala B. 2003. Bayesian inference of recent migration rates using multilocus genotypes. *Genetics*. 163(3):1177–1191.

Wright J.W., Vitt L.J. 1993. *Biology of whiptail lizards* (genus *Cnemidophorus*). Norman, OK: The Oklahoma Museum of Natural History.

Zheng X., Levine D., Shen J., Gogarten S.M., Laurie C., Weir B.S. 2012. A high-performance computing toolset for relatedness and principal component analysis of SNP data. *Bioinformatics*. 28(24):3326–3328.

Zhu J., Nakhleh L. 2018. Inference of species phylogenies from bi-allelic markers using pseudo-likelihood. *Bioinformatics*. 34:i376–i385.

Zweifel R.G. 1959. Variation in and distribution of lizards of western Mexico related to *Cnemidophorus sacki*. *Bull. Am. Mus. Nat. Hist.* 117:59–116.